

The Power Grid Library for Benchmarking AC Optimal Power Flow Algorithms

Contributors to the IEEE PES PGLib-OPF Task Force

Sogol Babaeinejad sarookolaee
Electrical and Computer Engineering
University of Wisconsin-Madison, WI, USA

Richard D. Christie
Electrical and Computer Engineering
University of Washington, WA, USA

Christopher DeMarco
Electrical and Computer Engineering
University of Wisconsin-Madison, WI, USA

Michael Ferris
Computer Sciences
University of Wisconsin-Madison, WI, USA

Scott Greene
Electrical and Computer Engineering
University of Wisconsin-Madison, WI, USA

Cédric Josz
Industrial Engineering and Operations Research
Columbia University, New York, NY, USA

Bernard Lesieurte
Electrical and Computer Engineering
University of Wisconsin-Madison, WI, USA

Daniel K. Molzahn
Electrical and Computer Engineering
Georgia Institute of Technology, GA, USA

Patrick Panciatici
Research and Development Division
Reseau de Transport d'Electricite (RTE), Paris, France

Jonathan Snodgrass
Electrical and Computer Engineering
University of Wisconsin-Madison, WI, USA

Adam Birchfield
Electrical and Computer Engineering
Texas A&M University, TX, USA

Carleton Coffrin*
Advanced Network Science Initiative
Los Alamos National Laboratory, NM, USA

Ruisheng Diao
AI & System Analytics
GEIRI North America, San Jose, CA

Stéphane Fliscounakis
Research and Development Division
Reseau de Transport d'Electricite (RTE), Paris, France

Renke Huang
Electricity Infrastructure Group
Pacific Northwest National Laboratory, Richland, WA, USA

Roman Korab
Electrical Engineering
Silesian University of Technology, Gliwice, Poland

Jean Maeght
Research and Development Division
Reseau de Transport d'Electricite (RTE), Paris, France

Thomas J. Overbye
Electrical and Computer Engineering
Texas A&M University, TX, USA

Byungwon Park
Computational Sciences and Engineering Division
Oak Ridge National Laboratory, Oak Ridge, TN, USA

Ray Zimmerman
Applied Economics and Management
Cornell University, Ithaca, NY, USA

The PGLib-OPF benchmarks are available at <https://github.com/power-grid-lib/pglib-opf>.

* Corresponding author cjc@lanl.gov.

Abstract—In recent years, the power systems research community has seen an explosion of novel methods for formulating the AC power flow equations. Consequently, benchmarking studies using the seminal AC Optimal Power Flow (AC-OPF) problem have emerged as the primary method for evaluating these emerging methods. However, it is often difficult to directly compare these studies due to subtle differences in the AC-OPF problem formulation as well as the network, generation, and loading data that are used for evaluation. To help address these challenges, this IEEE PES Task Force report proposes a standardized AC-OPF mathematical formulation and the PGLib-OPF networks for benchmarking AC-OPF algorithms. A motivating study demonstrates some limitations of the established network datasets in the context of benchmarking AC-OPF algorithms and a validation study demonstrates the efficacy of using the PGLib-OPF networks for this purpose. In the interest of scientific discourse and future additions, the PGLib-OPF benchmark library is open-access and all the of network data is provided under a creative commons license.

Index Terms—Nonlinear Optimization, Convex Optimization, AC Optimal Power Flow, Benchmarking

NOMENCLATURE

| | |
|--------------------------|--|
| N | - The set of buses in the network |
| G | - The set of generators in the network |
| E | - The set of <i>from</i> branches in the network |
| E^R | - The set of <i>to</i> branches in the network |
| i | - Imaginary number constant |
| e | - Exponential constant |
| $S = p + iq$ | - AC power |
| $V = v\angle\theta$ | - AC voltage |
| $Z = r + ix$ | - Branch impedance |
| $Y = g + ib$ | - Branch admittance |
| $T = t\angle\theta^t$ | - Branch transformer properties |
| $Y^s = g^s + ib^s$ | - Bus shunt admittance |
| v | - Nominal base voltage |
| b^c | - Line charging |
| s^u | - Branch apparent power limit |
| I^u | - Branch current magnitude limit |
| θ^Δ | - Voltage angle difference limit |
| $S^d = p^d + iq^d$ | - AC power demand |
| $S^g = p^g + iq^g$ | - AC power generation |
| c_0, c_1, c_2 | - Generation cost coefficients |
| $\Re(\cdot), \Im(\cdot)$ | - Real and imag. parts of a complex number |
| $ \cdot \angle \cdot$ | - Magnitude and angle of a complex number |
| $(\cdot)^*$ | - Conjugate of a complex number |
| x^l, x^u | - Lower and upper bounds of x , respectively |
| x | - A constant value |
| \hat{x} | - An estimation of x |
| μ | - Mean of a normal distribution |
| σ | - Standard deviation of a normal distribution |
| λ | - Rate of an exponential distribution |

I. INTRODUCTION

Over the last decade, power systems research has experienced an explosion in variations of the steady-state AC

power flow equations. These include approximations such as the LPAC [1], IV-Flow [2] and relaxations such as the Second-Order Cone (SOC) [3], Convex-DistFlow (CDF) [4], Quadratic Convex (QC) [5], [6], Semidefinite Programming (SDP) [7], and Moment / Sum-of-Squares Hierarchies [8]–[11], just to name a few. Surveys of the power flow relaxation and approximation literature are provided in [12]–[14]. Much of the excitement underlying this line of research was ignited when [15] demonstrated that the SDP relaxation could provide globally optimal solutions to a variety of the transmission system networks distributed with MATPOWER [16]. Combining these results with industrial-strength convex optimization tools (e.g., Gurobi [17], Cplex [18], Mosek [19]) promises efficient and reliable algorithms for a wide variety of applications in power systems such as optimal power flow [20]–[23], optimal transmission switching [24], and network expansion planning [25], just to name a few.

Independent of the specific problem domain or the power flow model under consideration, all of these novel methods require AC power network data for experimental validation and it is important that suitable data are used to validate these emerging techniques [26]. However, due to the sensitive nature of critical infrastructure, detailed real-world network data is often difficult to obtain, even under non-disclosure agreements. Consequently, many of the available power network datasets are over thirty years old (e.g. [27]), were originally designed for testing AC Power Flow algorithms, and lack the parameters needed for testing the AC Optimal Power Flow algorithms, e.g. branch thermal limits and generator cost functions. The lack of comprehensive and modern AC power network data has been recognized by the Advanced Research Projects Agency-Energy (ARPA-e) and the GRID DATA program [28] has resulted in a number of new network datasets, which are synthetically generated to match the statistics of real-world networks and provided as open-access.

To help improve the evaluation of AC-OPF algorithms, this IEEE PES Task Force report introduces the Power Grid Library for benchmarking the AC-OPF problem, PGLIB-OPF. PGLIB-OPF is a comprehensive collection of creative-commons AC transmission system networks curated in the MATPOWER data format with all of the data required for modeling the proposed AC-OPF problem. This report is a companion document to the PGLIB-OPF data. Section II begins with a detailed specification of the AC-OPF problem. Section III provides a brief overview of the established AC-OPF cases provided with MATPOWER and highlights some limitations in using these cases for benchmarking AC-OPF algorithms. Section IV provides a survey of known creative-commons transmission system network data and highlights the missing information in each network data source. Section V briefly introduces methods for addressing the missing information in these datasets. Section VI introduces the PGLIB-

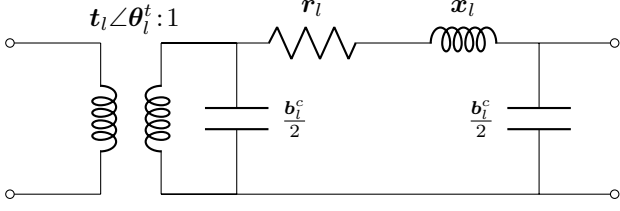


Fig. 1. II-circuit branch model with an ideal transformer. This is the branch model used by MATPOWER [16].

OPF networks and conducts a baseline validation study to demonstrate that they are suitable for benchmarking the AC-OPF problem. Section VII provides concluding remarks. An appendix summarizes some variants of the proposed AC-OPF model and discusses the additional data that may be necessary in order to make the PGLIB-OPF test cases applicable to other classes of power system optimization and control problems.

II. THE AC OPTIMAL POWER FLOW FORMULATION

Many variations of the AC-OPF problem are relevant to power system analysis. However, in accordance with PGLIB repository requirements, this section nominates a specific version of the AC-OPF problem for algorithmic benchmarking. The following mathematical model presents a variant of the AC-OPF problem that is often used in related AC-OPF publications (e.g. [1]–[5], [11], [15]) and is readily encoded in the MATPOWER network data format.

The proposed AC-OPF problem requires the following network parameters: a set of bus ids N ; a set of branch ids E with an arbitrary orientation; a set E^R that captures the reverse orientation of the branches; and a set of generator ids G . For each bus $i \in N$: the sets E_i and E_i^R indicate the subset of edges that are incident to that bus; the set G_i reflects the subset of generator ids that are connected to that bus; S_i^d is the constant power demand; \mathbf{Y}_i^s is the bus shunt admittance; and v_i^l, v_i^u indicate the operating range of the bus' voltage magnitude. For each generator $k \in G$: S_k^{gl}, S_k^{gu} indicate the generator's power injection range; and c_{2k}, c_{1k}, c_{0k} provide the coefficients of a quadratic active power cost function. For each branch $(l, i, j) \in E$: i and j are the *from* and *to* buses respectively and l is the branch id; the series admittance, line charge, and transformer parameters are given by $\mathbf{Y}_l, b_l^c, \mathbf{T}_l$ respectively; the branch's thermal limit is given by s_l^u ; and the branch voltage angle difference range is $\theta_l^{\Delta l}, \theta_l^{\Delta u}$. Lastly, a voltage angle reference bus $ref \in N$ is specified. Most of these parameters are specified directly in a MATPOWER data file. However, the following parameters need to be computed from the raw data as follows,

$$\mathbf{Y}_l = \mathbf{Z}_l^{-1} = \frac{\mathbf{r}_l}{\mathbf{r}_l^2 + \mathbf{x}_l^2} - i \frac{\mathbf{x}_l}{\mathbf{r}_l^2 + \mathbf{x}_l^2} \quad (1a)$$

$$\mathbf{T}_l = t_l \cos(\theta_l^t) + i t_l \sin(\theta_l^t) \quad (1b)$$

Model 1 The AC Optimal Power Flow Problem (AC-OPF)

variables:

$$S_k^g \quad \forall k \in G$$

$$V_i \quad \forall i \in N$$

$$S_{lij} \quad \forall (l, i, j) \in E \cup E^R$$

$$\text{minimize: } \sum_{k \in G} c_{2k} (\Re(S_k^g))^2 + c_{1k} \Re(S_k^g) + c_{0k} \quad (2a)$$

subject to:

$$\angle V_{ref} = 0 \quad (2b)$$

$$S_k^{gl} \leq S_k^g \leq S_k^{gu} \quad \forall k \in G \quad (2c)$$

$$v_i^l \leq |V_i| \leq v_i^u \quad \forall i \in N \quad (2d)$$

$$\sum_{k \in G_i} S_k^g - S_i^d - \mathbf{Y}_i^s |V_i|^2 = \sum_{(l, i, j) \in E_i \cup E_i^R} S_{lij} \quad \forall i \in N \quad (2e)$$

$$S_{lij} = \left(\mathbf{Y}_l^* - i \frac{b_l^c}{2} \right) \frac{|V_i|^2}{|\mathbf{T}_l|^2} - \mathbf{Y}_l^* \frac{V_i V_j^*}{\mathbf{T}_l} \quad \forall (l, i, j) \in E \quad (2f)$$

$$S_{lji} = \left(\mathbf{Y}_l^* - i \frac{b_l^c}{2} \right) |V_j|^2 - \mathbf{Y}_l^* \frac{V_i^* V_j}{\mathbf{T}_l^*} \quad \forall (l, i, j) \in E \quad (2g)$$

$$|S_{lij}| \leq s_l^u \quad \forall (l, i, j) \in E \cup E^R \quad (2h)$$

$$\theta_l^{\Delta l} \leq \angle(V_i V_j^*) \leq \theta_l^{\Delta u} \quad \forall (l, i, j) \in E \quad (2i)$$

Figure 1 shows the circuit model used to represent each branch.

Model 1 presents the AC-OPF problem as a non-convex nonlinear mathematical program over complex values and variables. A detailed description of the model's notation and derivation can be found in [5]. The objective function (2a) strives to minimize the cost of active power injections. Constraint (2b) fixes the voltage angle of the reference bus. Constraint (2c) sets the generator injection limits and constraint (2d) sets the bus voltage magnitude limits. Constraint (2e) captures the nodal power balance and constraints (2f)–(2g) ensure that the branch power flows are consistent with Ohm's Law. Finally, constraints (2h) and (2i) capture the branch thermal and voltage angle difference limits. It is important to note that solving Model 1 is NP-Hard [29] in general, even if the network has a tree topology [30]. Consequently, it is expected that solution methods for Model 1 will exhibit a wide variety of quality-runtime tradeoffs and will be specialized to different classes of inputs.

III. MOTIVATION

To motivate the need for a careful curation of the network data in PGLIB-OPF, this section conducts a preliminary study of thirty-five AC transmission system datasets that are distributed with MATPOWER v6.0 [16], [48]. The *optimality gap* measure is used as a simple and preliminary test of AC-OPF difficulty, as one expects that challenging cases will exhibit a large optimality gap. Given a feasible solution to the AC-OPF problem and the solution to a convex relaxation,

TABLE I
AC-OPF OPTIMALITY GAPS ON NETWORK DATASETS DISTRIBUTED WITH MATPOWER V6.0.

| Test Case | <i>N</i> | <i>E</i> | \$/h | Gap (%) | Runtime (seconds) | |
|------------------|----------|----------|------------|---------|-------------------|-----|
| | | | AC | SOC | AC | SOC |
| case5 | 5 | 6 | 1.7552e+04 | 14.55 | <1 | <1 |
| case6ww | 6 | 11 | 3.1440e+03 | 0.63 | <1 | <1 |
| case9 | 9 | 9 | 5.2967e+03 | 0.01 | <1 | <1 |
| case9target | 9 | 9 | n.s. | inf. | <1 | <1 |
| case14 | 14 | 20 | 8.0815e+03 | 0.08 | <1 | <1 |
| case24_ieee_rts | 24 | 38 | 6.3352e+04 | 0.02 | <1 | <1 |
| case30 | 30 | 41 | 5.7689e+02 | 0.58 | <1 | <1 |
| case_ieee30 | 30 | 41 | 8.9061e+03 | 0.05 | <1 | <1 |
| case39 | 39 | 46 | 4.1864e+04 | 0.03 | <1 | <1 |
| case57 | 57 | 80 | 4.1738e+04 | 0.07 | <1 | <1 |
| case89pegase | 89 | 210 | 5.8198e+03 | 0.17 | <1 | <1 |
| case118 | 118 | 186 | 1.2966e+05 | 0.25 | <1 | <1 |
| case145 | 145 | 453 | n.s. | inf. | 14 | 7 |
| case_illinois200 | 200 | 245 | 3.6748e+04 | 0.02 | <1 | <1 |
| case300 | 300 | 411 | 7.1973e+05 | 0.15 | <1 | <1 |
| case1354pegase | 1354 | 1991 | 7.4069e+04 | 0.08 | 4 | 5 |
| case1951 rte | 1951 | 2596 | 8.1738e+04 | 0.08 | 17 | 26 |
| case2383wp | 2383 | 2896 | 1.8685e+06 | 1.05 | 9 | 6 |
| case2736sp | 2736 | 3504 | 1.3079e+06 | 0.30 | 8 | 5 |
| case2737sop | 2737 | 3506 | 7.7763e+05 | 0.26 | 6 | 4 |
| case2746wop | 2746 | 3514 | 1.2083e+06 | 0.37 | 7 | 4 |
| case2746wp | 2746 | 3514 | 1.6318e+06 | 0.33 | 7 | 5 |
| case2848rte | 2848 | 3776 | 5.3022e+04 | 0.08 | 46 | 7 |
| case2868rte | 2868 | 3808 | 7.9795e+04 | 0.07 | 28 | 8 |
| case2869pegase | 2869 | 4582 | 1.3400e+05 | 0.09 | 9 | 58 |
| case3012wp | 3012 | 3572 | 2.5917e+06 | 0.78 | 12 | 6 |
| case3120sp | 3120 | 3693 | 2.1427e+06 | 0.54 | 11 | 6 |
| case3375wp | 3374 | 4161 | 7.4120e+06 | 0.26 | 13 | 98 |
| case6468rte | 6468 | 9000 | 8.6829e+04 | 0.23 | 67 | 226 |
| case6470rte | 6470 | 9005 | 9.8345e+04 | 0.17 | 61 | 105 |
| case6495rte | 6495 | 9019 | 1.0628e+05 | 0.45 | 44 | 239 |
| case6515rte | 6515 | 9037 | 1.0980e+05 | 0.38 | 45 | 36 |
| case9241pegase | 9241 | 16049 | 3.1591e+05 | 1.75 | 61 | 230 |
| case13659pegase | 13659 | 20467 | 3.8611e+05 | 1.52 | 228 | 215 |

the optimality gap is defined as the relative difference between the objective values of the feasible solution and the relaxation:

$$\frac{\text{AC Heuristic} - \text{AC Relaxation}}{\text{AC Heuristic}} \quad (3)$$

There are a wide variety of both AC heuristics (i.e., methods for obtaining feasible solutions to AC OPF problems [21]–[23]) and convex relaxation techniques [12]–[14]. In the interest of simplicity, this preliminary study will use a nonlinear optimization solver that converges to a KKT point as a heuristic for finding AC feasible solutions and a simple Second-Order Cone (SOC) relaxation [3] for providing objective bounds. All of the results were computed using IPOPT 3.12 [49] with the HSL [50] linear algebra library on a server with two 2.10GHz Intel CPU and 128GB of RAM. PowerModels.jl v0.9 [51] was

used to formulate and solve both mathematical programs.

The results of this study are presented in Table I. The data highlights two core points: (1) By-in-large the optimality gaps are less than 1%. Although a large optimality gap is not a necessary condition for AC-OPF hardness, it provides a good indication of a challenging instance. This work will demonstrate that much more significant gaps are possible, providing a significant increase in the variety of network cases for AC-OPF algorithm benchmarking; (2) No feasible solution was found in two cases, case9target and case145. This could suggest that these cases are challenging for AC heuristics. However, the SOC relaxation provides a numerical proof that

TABLE II
A SURVEY OF TRANSMISSION SYSTEM DATA SOURCES*

| Name | Original Source | Generator Injection Limits | Generator Costs | Thermal Limits |
|--|-----------------|----------------------------|-----------------|----------------|
| Publication Test Cases | | | | |
| 3-Bus | [31] | [31] | [31] | [31] |
| case5 | [32] | [32] | [32] | — |
| case30-as | [33] | [33] | [33] | [33] |
| case30-fsr | [33] | [34] | [34] | [33] |
| case39 | [35] | [35], [36] | [37] | [38] |
| IEEE Power Flow Test Cases | | | | |
| 14 Bus | [27] | — | — | — |
| 30 Bus | [27] | — | — | — |
| 57 Bus | [27] | — | — | — |
| 118 Bus | [27] | — | — | — |
| 300 Bus | [27] | — | — | — |
| IEEE Dynamic Test Cases | | | | |
| 17 Generator | [27] | — | — | — |
| IEEE Reliability Test Systems (RTS) | | | | |
| RTS-79 | [39] | [39] | [39], [40] | [39] |
| RTS-96 | [41] | [39] | [40] | [39] |
| Polish Test Cases | | | | |
| case2383wp | [16] | [16] | [16] | [16] |
| case2736sp | [16] | [16] | [16] | [16] |
| case2737sop | [16] | [16] | [16] | [16] |
| case2746wop | [16] | [16] | [16] | [16] |
| case2746wp | [16] | [16] | [16] | [16] |
| case3012wp | [16] | [16] | [16] | — |
| case3120sp | [16] | [16] | [16] | — |
| case3375wp | [16] | — | [16] | — |
| PEGASE Test Cases | | | | |
| case89pegase | [42] | [42] | — | [42], partial |
| case1354pegase | [42] | [42] | — | [42], partial |
| case2869pegase | [42] | [42] | — | [42], partial |
| case9241pegase | [42] | [42] | — | [42], partial |
| case13659pegase | [42] | [42] | — | [42], partial |
| RTE Test Cases | | | | |
| case1888rte | [42] | [42] | — | [42], partial |
| case1951rte | [42] | [42] | — | [42], partial |
| case2848rte | [42] | [42] | — | [42], partial |
| case2868rte | [42] | [42] | — | [42], partial |
| case6468rte | [42] | [42] | — | [42], partial |
| case6470rte | [42] | [42] | — | [42], partial |
| case6495rte | [42] | [42] | — | [42], partial |
| case6515rte | [42] | [42] | — | [42], partial |
| Texas A&M University Test Cases | | | | |
| ACTIVSg200 | [43] | [43] | [43] | [43] |
| ACTIVSg500 | [43] | [43] | [43] | [43] |
| ACTIVSg2000 | [43] | [43] | [43] | [43] |
| ACTIVSg10k | [43] | [43] | [43] | [43] |
| Sustainable Data Evolution Technology Test Cases | | | | |
| SDET 500 | [44] | [44] | — | [44] |
| SDET 2000 | [44] | [44] | — | [44] |
| SDET 3000 | [44] | [44] | — | [44] |
| SDET 4000 | [44] | [44] | — | [44] |
| Grid Optimization Competition Test Cases | | | | |
| 179 Bus | [45] | [45] | — | — |
| Power Systems Engineering Research Center Test Cases | | | | |
| WECC 240 Bus | [46], [47] | [47] | [47] | [47] |

* - only creative commons data sources were considered

these cases have no feasible AC-OPF solution,¹ suggesting that data quality is the source of infeasibility and not algorithmic difficulty. Overall, this simplistic study demonstrates some of the shortcomings of focusing exclusively on the network data that is distributed with MATPOWER v6.0 for benchmarking AC-OPF algorithms. The careful curation of AC network data developed in the following sections results in modified network datasets featuring significant optimality gaps, which will help to emphasize the differences between various AC-OPF solution methods.

IV. PUBLICLY AVAILABLE NETWORK DATA

In the interest of curating a comprehensive collection of AC-OPF networks, we begin with a survey of available network datasets. To the best of our knowledge, Table II summarizes all of the readily available transmission system datasets.² A careful investigation of these datasets reveals that very few networks include all of the data required to study Model 1. Table II highlights the source of, or lack of, generation capacity limits, generation cost functions, and branch thermal limits in these datasets. Cells containing “—” indicate missing data that must be added before the network will be suitable for benchmarking Model 1. To address the information that is missing in these datasets, the next section reviews a number of data-driven models that can be used to fill in these gaps.

A. Network Omissions

Some notable networks have not been included in Table II for the following reasons.

1) IEEE 30 Bus “New England” Dynamic Test System:

This test case is nearly identical to the IEEE 30 test case and would not bring additional value to the proposed collection of cases.

2) IEEE 50 Generator Dynamic Test System:

In its specified state, this test case does not converge to an AC power flow solution. However, if the active generation upper bounds are increased to 1.5 times their given value and voltage bounds are set to 1 ± 0.16 , then a solution can be obtained. This solution still exhibits significant voltage drops, atypical of other networks. Many of the lines in this network have negative r and x values, which is likely the result of a network reduction procedure. Also, the size of the generating units are one or two orders of magnitude larger than any documented generation unit in the U.S., which suggests that these “generators” may actually be modeling imports and exports of power. Since many of these characteristics are atypical compared to the other test cases, this network is omitted.

¹That is, there does not exist an assignment of the variables that can simultaneously satisfy all of the constraints in Model 1.

²Only creative commons datasets were considered to comply with PGLIB data requirements.

V. DATA DRIVEN MODELS

Ideally, the data missing from Table II would be incorporated by returning to the original network design documents and extracting the required information, such as a generator’s nameplate capacity and line conductor specifications. Unfortunately, due to the age or the synthetic nature of these test cases, this approach to data completion is impractical. This work proposes to leverage publicly available data sources to build data-driven models that can complete the missing data. Such models may not reflect any specific real-world network, but at least they will reflect many of the statistical features found in realistic networks. As identified in Section IV, the key pieces of missing data are generator injection limits, generation costs functions, and branch thermal limits. The rest of this section reviews several data-driven models proposed in [52], which can be used to fill the gaps in these networks.

A. Generator Models

Most AC transmission datasets are brief in their description of the generation units. Typically, only the active power injection limits, reactive power injection limits, and a specific generation dispatch point are provided. A notable omission is an active power generation cost function, which is critical in formulating the objective in Model 1. Two key observations can be used to address the limited information on generation units: (1) The U.S. Energy Information Administration (EIA) collects extensive data on generation units throughout the United States. Two reports are particularly useful to this work, the detailed generator data (EIA-860 2012 [53]) and state fuel cost data (SEDS [54]); (2) The bulk of a generator’s properties are driven by its mechanical design, which is in turn significantly influenced by its fuel type. This work begins by developing a data-driven model for generators by assigning them a fuel category. Once a fuel category is determined, probabilistic models for both fuel costs and power injection limits can be derived from publicly available data sources. In the interest of simplicity, this work focuses on the four primary dispatchable fuel types, Petroleum (PEL), Natural Gas (NG), Coal (COW), and Nuclear Fuel (NUC).

1) *The Generation Fuel Category Model:* Assuming that a generator’s active power injection limit (i.e. $\Re(\mathbf{S}^{g_u})$) is a sufficient proxy for its nameplate capacity, one can use the empirical distribution presented in Figure 2 for making a probabilistic guess of the fuel type of a given generation unit. The fuel category classifier is built by selecting the corresponding nameplate capacity bin in Figure 2 and rolling a weighted die to select the fuel type.

One important point is the identification of synchronous condensers. In Model 1 such devices are not explicitly identified but are modeled as generators with no active generation capabilities. To identify such devices, one can introduce a new

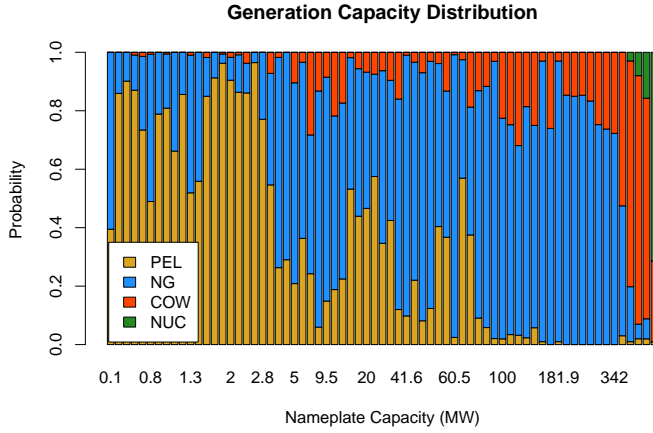


Fig. 2. An Empirical Distribution of Generation Fuel Categories by Nameplate Capacity.

fuel category (e.g. SYNC), and any generator with active generation upper and lower bounds of 0 is assigned this category. The empirical distribution shown in Figure 2 combined with this special case forms the generation fuel classification model (**GF-Stat**).

2) *Generation Capacity Models*: Some AC transmission system datasets lack reasonable generation injection limits, especially in cases that were originally designed for benchmarking AC Power Flow algorithms. Two simple generation capability models are developed to address such cases.

a) *Active Generation Capability*: An investigation of the nameplate capacities of each fuel type in [52] revealed that an exponential distribution is a suitable model for PEL, NG, and COW generators, while a normal distribution is suitable for NUC generators. The parameters from maximum likelihood estimation of these distributions are presented in Table III. Using these distributions the active generation capacity model (**AG-Stat**) is constructed as follows. Given a fuel category f and an active generation upper limit or present output $\mathfrak{R}(S^g)$, the fuel category nameplate capacity distribution is sampled as p^{gu} , until $p^{gu} > \mathfrak{R}(S^g)$. Then the maximum active power generation capacity is updated to the sampled value, i.e. $\mathfrak{R}(S^{gu}) = p^{gu}$.

TABLE III
DISTRIBUTION PARAMETERS FOR GENERATOR CAPACITY MODELS.

| Fuel Type | Nameplate Capacity (MW) | |
|-----------|-------------------------|--|
| | $\hat{\lambda}$ | |
| PEL | 0.023254 | |
| NG | 0.009188 | |
| COW | 0.003201 | |

| Fuel Type | Nameplate Capacity (MW) | |
|-----------|-------------------------|----------------|
| | $\hat{\mu}$ | $\hat{\sigma}$ |
| NUC | 1044.56 | 219.27 |

b) *Reactive Generation Capabilities*: In synchronous machines, reactive generation capabilities are tightly coupled with active generation capabilities. Lacking detailed information about the generator's specifications it is observed in [52] that the reactive power capability of a synchronous machine is roughly $\pm 50\%$ of its nameplate capacity leading to the **RG-AM50** model. This model assumes the given reactive power bounds are accurate, unless they exceed 50% of the nameplate capacity, in which case, they are reduced to $\pm 50\%$ of the nameplate capacity. This provides a pessimistic model of the generator's capabilities.

3) *Generation Cost Model*: Observing the simplicity of the cost function in Model 1, this work proposes to focus on the marginal costs of power generation in an idealized non-competitive environment. Fuel price information is available in the "Primary Energy, Electricity, and Total Energy Price Estimates, 2012" in the SEDS dataset [54]. In [52] it was observed that for the fuel categories of interest, the fuel costs are roughly normally distributed, with the parameters specified in Table IV. Using these distributions the model for generation costs (**AC-Stat**) is built as follows. The fuel cost parameters from Table IV are assumed to be representative of the price variations across the various generating units, so that, given a fuel category, one simply draws a sample from the associated normal distribution to produce a linear fuel cost value (\$/BTU) for that generator. The conversion from heat energy input (BTU) to electrical energy output (MWh) depends on a generator's *heat rate*, which differs based on the efficiency of the generating plant. Representative heat rate values are adopted from 2016 EIA data [55].

TABLE IV
GENERATOR COST MODEL.

| Fuel Category | SEDS Label | Cost (\$/MWh) | |
|---------------|---------------------|---------------|----------------|
| | | $\hat{\mu}$ | $\hat{\sigma}$ |
| PEL | Distillate Fuel Oil | 111.3398 | 9.6736 |
| NG | Natural Gas | 34.2731 | 10.9810 |
| COW | Coal | 24.7919 | 8.0866 |
| NUC | Nuclear Fuel | 7.2504 | 0.7534 |

B. Branch Thermal Limit Models

Determining a transmission line's operational thermal rating is an intricate task that combines a wide variety of information such as the conductor's design, location, age and the season of the year. Unfortunately, this information is unavailable in all of the network datasets presented in Table II. The only available branch parameters are the impedance ($Z = r + ix$ p.u.), line charge (b^c p.u.), and often the nominal voltage (v) on the connecting buses. This work leverages two models for producing reasonable thermal limits, a data-driven approach and an arithmetic approach leveraging other model parameters.

1) *A Statistical Model*: After reviewing a number of network datasets with realistic thermal limits, [52] concluded that the following exponential model was reasonable estimator of thermal limits when the impedance ($Z = r + ix$ p.u.) and nominal voltage (v) is known,

$$s^u = v e^{-5.0886} \left(\frac{x}{r}\right)^{0.4772} \quad (4)$$

This model is referred to as **TL-Stat**. The intuition of the model is that the ratio of resistance to impedance provides some insight into the branch's conductor type and configuration, since this ratio should be independent of the line length.

2) *A Reasonable Upper Bound*: Although the statistical model for branch thermal limits is quite useful, it cannot be applied in cases where data for r , x , or v is missing. Notable examples include: transformers, where the nominal voltage value differs on both sides of the line, and ideal lines, which do not have an r value. For these cases, it is helpful to have an alternate method for producing reasonable thermal limits.

Given that Model 1 includes reasonable bounds on $|V|$ and θ^Δ , a reasonable thermal limit can be computed as follows. For a branch $(l, i, j) \in E$, let $\theta_l^{\Delta m} = \max(|\theta_l^{\Delta l}|, |\theta_l^{\Delta u}|)$. A reasonable value for s_l^u is

$$(s_l^u)^2 = (v_i^u)^2 |Y_l|^2 ((v_i^u)^2 + (v_j^u)^2 - 2v_i^u v_j^u \cos(\theta_l^{\Delta m})) \quad (5)$$

This model is referred to as **TL-UB** and a more detailed discussion can be found in [52].

C. Voltage Angle Difference Bounds

Voltage angle difference bounds are often used as a proxy for capturing voltage angle stability limits on long transmissions lines [56]. Unfortunately, no available network datasets include detailed information for these bounds, which are specified in Model 1. To fill this gap all of the PGLIB-OPF models are given generous voltage angle difference bound of $\theta^{\Delta l} = -30^\circ$, $\theta^{\Delta u} = 30^\circ$, which are easily justified by practical voltage stability requirements [56] and do not impact the best-known solution of any available network. It is important to emphasize that a voltage angle difference bound of 30° is generous enough to be subsumed by the thermal limits provided with all of the networks considered here. Still, even this generous value has significant implications for the development of power system optimization methods (e.g. [1], [5], [6], [57], [58]).

VI. THE PGLIB-OPF NETWORKS

Leveraging the proposed models for completing the missing data in Table II, the PGLIB-OPF networks are developed. Table V summarizes which models are used to convert the base network data into PGLIB-OPF networks.

A. Results

To verify the usefulness of the proposed PGLIB-OPF networks for benchmarking AC-OPF algorithms, the study from Section III is revisited. PowerModels.jl v0.8 [51] was used to formulate Model 1 and its Second-Order Cone (SOC) relaxation [3], [5] and both models were solved with IPOPT 3.12 [49] using the HSL [50] linear algebra library on a server with two 2.10GHz Intel CPU and 128GB of RAM.

Table VI presents the results of the base PGLIB-OPF networks, which are called the Typical Operating Conditions (TYP) cases. Many of the optimality gaps have remained small (i.e. below 1%). However, a number of networks do exhibit significant optimality gaps, such as `pglib_opf_case5_pjm`, `pglib_opf_case30_ieee`, `pglib_opf_case162_ieee_dtc`, `pglib_opf_case500_tamu`, `pglib_opf_case6495_rte`, and `pglib_opf_case6515_rte`. This suggests that at least a subset of these cases are interesting for benchmarking AC-OPF algorithms.

B. Building More Challenging Test Cases

The typical operating conditions networks presented in Table VI provide a suitable start for benchmarking AC-OPF algorithms. However, it is worthwhile to explore if even more challenging test cases can be devised. To that end, PGLIB-OPF includes two variants of the base PGLIB-OPF networks that exhibit even more extreme optimality gaps, the Active Power Increase (API) and Small Angle Difference (SAD) cases.

Active Power Increase (API) Cases: It was observed in [59], [60] that power flow congestion is a key feature of interesting AC Optimal Transmission Switching test cases. Inspired by this observation, the following Active Power Increase (API) PGLIB-OPF networks are proposed. For each of the standard PGLIB-OPF networks, an optimization problem is solved, which increases the active power demands proportionally throughout the network until the branch thermal limits are binding. Once a maximal increase in active power demand is determined, the statistical models are applied to appropriately update the other network parameters (e.g. generator capabilities and cost functions). The results of the API networks are presented in Table VII. As expected, the optimality gaps in these networks have increased significantly with 60% of cases having optimality gaps above 1% and eight cases with optimality gaps above 10%. This suggests that many of these cases will be useful for benchmarking AC-OPF algorithms.

Small Angle Difference (SAD) Cases: A second approach to modifying the PGLIB-OPF networks is inspired by recent lines of research [1], [5], [6], [57] that indicate voltage angle difference bounds can have significant impacts on power system optimization approaches. To emphasize these impacts, the following Small Angle Difference (SAD) PGLIB-OPF networks are proposed. For each of the standard PGLIB-

TABLE V
PGLIB-OPF INSTANCE GENERATION DETAILS

| PGLIB Name | Original Name | Model | | | | | Voltage Angle Diff. Bound |
|--|-----------------|-------------|---------------|-----------|---------------|---|---------------------------|
| | | Active Gen. | Reactive Gen. | Gen. Cost | Thermal Limit | | |
| Publication Test Cases | | | | | | | |
| pglib_opf_case3_lmbd | 3-Bus | — | — | — | — | — | 30° |
| pglib_opf_case5_pjm | case5 | — | — | — | TL-Stat | — | 30° |
| pglib_opf_case30_as | 30 Bus-as | — | — | — | — | — | 30° |
| pglib_opf_case30_fsr | 30 Bus-fsr | — | — | — | — | — | 30° |
| pglib_opf_case39_epri | case39 | — | — | — | — | — | 30° |
| IEEE Power Flow Test Cases | | | | | | | |
| pglib_opf_case14_ieee | 14 Bus | AG-Stat | RG-AM50 | AC-Stat | TL-Stat | — | 30° |
| pglib_opf_case30_ieee | 30 Bus | AG-Stat | RG-AM50 | AC-Stat | TL-Stat | — | 30° |
| pglib_opf_case57_ieee | 57 Bus | AG-Stat | RG-AM50 | AC-Stat | TL-Stat | — | 30° |
| pglib_opf_case118_ieee | 118 Bus | AG-Stat | RG-AM50 | AC-Stat | TL-Stat | — | 30° |
| pglib_opf_case300_ieee | 300 Bus | AG-Stat | RG-AM50 | AC-Stat | TL-UB | — | 30° |
| IEEE Dynamic Test Cases | | | | | | | |
| pglib_opf_case162_ieee_dtc | 17 Generator | AG-Stat | RG-AM50 | AC-Stat | TL-Stat | — | 30° |
| IEEE Reliability Test Systems (RTS) | | | | | | | |
| pglib_opf_case24_ieee_rts | RTS-79 | — | — | — | — | — | 30° |
| pglib_opf_case73_ieee_rts | RTS-96 | — | — | — | — | — | 30° |
| Polish Test Cases | | | | | | | |
| pglib_opf_case2383wp_mp | case2383wp | — | — | — | — | — | 30° |
| pglib_opf_case2736sp_mp | case2736sp | — | — | — | — | — | 30° |
| pglib_opf_case2737sop_mp | case2737sop | — | — | — | — | — | 30° |
| pglib_opf_case2746wop_mp | case2746wop | — | — | — | — | — | 30° |
| pglib_opf_case2746wp_mp | case2746wp | — | — | — | — | — | 30° |
| pglib_opf_case3012wp_mp | case3012wp | — | — | — | TL-Stat | — | 30° |
| pglib_opf_case3120sp_mp | case3120sp | — | — | — | TL-Stat | — | 30° |
| pglib_opf_case3375wp_mp | case3375wp | — | RG-AM50 | — | TL-Stat | — | 30° |
| PEGASE Test Cases | | | | | | | |
| pglib_opf_case89_pegase | case89pegase | — | — | AC-Stat | TL-UB | — | 30° |
| pglib_opf_case1354_pegase | case1354pegase | — | — | AC-Stat | TL-UB | — | 30° |
| pglib_opf_case2869_pegase | case2869pegase | — | — | AC-Stat | TL-UB | — | 30° |
| pglib_opf_case9241_pegase | case9241pegase | — | — | AC-Stat | TL-UB | — | 30° |
| pglib_opf_case13659_pegase | case13659pegase | — | — | AC-Stat | TL-UB | — | 30° |
| RTE Test Cases | | | | | | | |
| pglib_opf_case1888_rte | case1888rte | — | — | AC-Stat | TL-UB | — | 30° |
| pglib_opf_case1951_rte | case1951rte | — | — | AC-Stat | TL-UB | — | 30° |
| pglib_opf_case2848_rte | case2848rte | — | — | AC-Stat | TL-UB | — | 30° |
| pglib_opf_case2868_rte | case2868rte | — | — | AC-Stat | TL-UB | — | 30° |
| pglib_opf_case6468_rte | case6468rte | — | — | AC-Stat | TL-UB | — | 30° |
| pglib_opf_case6470_rte | case6470rte | — | — | AC-Stat | TL-UB | — | 30° |
| pglib_opf_case6495_rte | case6495rte | — | — | AC-Stat | TL-UB | — | 30° |
| pglib_opf_case6515_rte | case6515rte | — | — | AC-Stat | TL-UB | — | 30° |
| Texas A&M University Test Cases | | | | | | | |
| pglib_opf_case200_tamu | ACTIVSg200 | — | — | — | — | — | 30° |
| pglib_opf_case500_tamu | ACTIVSg500 | — | — | — | — | — | 30° |
| pglib_opf_case2000_tamu | ACTIVSg2000 | — | — | — | — | — | 30° |
| pglib_opf_case10000_tamu | ACTIVSg10k | — | — | — | — | — | 30° |
| Sustainable Data Evolution Technology Test Cases | | | | | | | |
| pglib_opf_case588_sdet | SDET 500 | — | — | AC-Stat | — | — | 30° |
| pglib_opf_case2316_sdet | SDET 2000 | — | — | AC-Stat | — | — | 30° |
| pglib_opf_case2853_sdet | SDET 3000 | — | — | AC-Stat | — | — | 30° |
| pglib_opf_case4661_sdet | SDET 4000 | — | — | AC-Stat | — | — | 30° |
| Grid Optimization Competition Test Cases | | | | | | | |
| pglib_opf_case179_goc | 179 Bus | — | — | AC-Stat | TL-UB | — | 30° |
| Power Systems Engineering Research Center Test Cases | | | | | | | |
| pglib_opf_case240_psrec | WECC 240 Bus | — | — | AC-Stat | TL-UB | — | 30° |

TABLE VI
AC-OPF BOUNDS ON PGLIB-OPF TYP NETWORKS.

| Test Case | <i>N</i> | <i>E</i> | \$/h | Gap (%) | Runtime (sec.) | |
|------------------------------------|----------|----------|------------|---------|----------------|-----|
| | | | AC | SOC | AC | SOC |
| Typical Operating Conditions (TYP) | | | | | | |
| pglib_opf_case3_lmbd | 3 | 3 | 5.8126e+03 | 1.32 | <1 | <1 |
| pglib_opf_case5_pjm | 5 | 6 | 1.7552e+04 | 14.55 | <1 | <1 |
| pglib_opf_case14_ieee | 14 | 20 | 2.1781e+03 | 0.11 | <1 | <1 |
| pglib_opf_case24_ieee_rts | 24 | 38 | 6.3352e+04 | 0.02 | <1 | <1 |
| pglib_opf_case30_as | 30 | 41 | 8.0313e+02 | 0.06 | <1 | <1 |
| pglib_opf_case30_fsr | 30 | 41 | 5.7577e+02 | 0.39 | <1 | <1 |
| pglib_opf_case30_ieee | 30 | 41 | 8.2085e+03 | 18.84 | <1 | <1 |
| pglib_opf_case39_epri | 39 | 46 | 1.3842e+05 | 0.56 | <1 | <1 |
| pglib_opf_case57_ieee | 57 | 80 | 3.7589e+04 | 0.16 | <1 | <1 |
| pglib_opf_case73_ieee_rts | 73 | 120 | 1.8976e+05 | 0.04 | <1 | <1 |
| pglib_opf_case89_pegase | 89 | 210 | 1.0729e+05 | 0.75 | <1 | <1 |
| pglib_opf_case118_ieee | 118 | 186 | 9.7214e+04 | 0.91 | <1 | <1 |
| pglib_opf_case162_ieee_dtc | 162 | 284 | 1.0808e+05 | 5.95 | <1 | <1 |
| pglib_opf_case179_goc | 179 | 263 | 7.5427e+05 | 0.16 | <1 | <1 |
| pglib_opf_case200_tamu | 200 | 245 | 2.7558e+04 | 0.01 | <1 | <1 |
| pglib_opf_case240_psenc | 240 | 448 | 3.3297e+06 | 2.78 | 4 | 2 |
| pglib_opf_case300_ieee | 300 | 411 | 5.6522e+05 | 2.63 | <1 | <1 |
| pglib_opf_case500_tamu | 500 | 597 | 7.2578e+04 | 5.39 | <1 | <1 |
| pglib_opf_case588_sdet | 588 | 686 | 3.1314e+05 | 2.14 | <1 | <1 |
| pglib_opf_case1354_pegase | 1354 | 1991 | 1.2588e+06 | 1.57 | 5 | 3 |
| pglib_opf_case1888_rte | 1888 | 2531 | 1.4025e+06 | 2.05 | 11 | 48 |
| pglib_opf_case1951_rte | 1951 | 2596 | 2.0856e+06 | 0.14 | 20 | 6 |
| pglib_opf_case2000_tamu | 2000 | 3206 | 1.2285e+06 | 0.21 | 11 | 3 |
| pglib_opf_case2316_sdet | 2316 | 3017 | 1.7753e+06 | 1.80 | 8 | 5 |
| pglib_opf_case2383wp_k | 2383 | 2896 | 1.8682e+06 | 1.04 | 9 | 6 |
| pglib_opf_case2736sp_k | 2736 | 3504 | 1.3080e+06 | 0.31 | 8 | 5 |
| pglib_opf_case2737sop_k | 2737 | 3506 | 7.7773e+05 | 0.27 | 7 | 4 |
| pglib_opf_case2746wop_k | 2746 | 3514 | 1.2083e+06 | 0.37 | 7 | 4 |
| pglib_opf_case2746wp_k | 2746 | 3514 | 1.6317e+06 | 0.33 | 8 | 5 |
| pglib_opf_case2848_rte | 2848 | 3776 | 1.2866e+06 | 0.13 | 20 | 8 |
| pglib_opf_case2853_sdet | 2853 | 3921 | 2.0524e+06 | 0.91 | 11 | 7 |
| pglib_opf_case2868_rte | 2868 | 3808 | 2.0096e+06 | 0.10 | 18 | 9 |
| pglib_opf_case2869_pegase | 2869 | 4582 | 2.4628e+06 | 1.01 | 15 | 8 |
| pglib_opf_case3012wp_k | 3012 | 3572 | 2.6008e+06 | 1.03 | 11 | 9 |
| pglib_opf_case3120sp_k | 3120 | 3693 | 2.1457e+06 | 0.55 | 10 | 6 |
| pglib_opf_case3375wp_k | 3374 | 4161 | 7.4382e+06 | 0.55 | 13 | 7 |
| pglib_opf_case4661_sdet | 4661 | 5997 | 2.2513e+06 | 1.99 | 18 | 13 |
| pglib_opf_case6468_rte | 6468 | 9000 | 2.0697e+06 | 1.13 | 71 | 30 |
| pglib_opf_case6470_rte | 6470 | 9005 | 2.2376e+06 | 1.76 | 41 | 27 |
| pglib_opf_case6495_rte | 6495 | 9019 | 3.0678e+06 | 15.11 | 76 | 28 |
| pglib_opf_case6515_rte | 6515 | 9037 | 2.8255e+06 | 6.40 | 62 | 25 |
| pglib_opf_case9241_pegase | 9241 | 16049 | 6.2431e+06 | 2.54 | 59 | 39 |
| pglib_opf_case10000_tamu | 10000 | 12706 | 2.4859e+06 | 0.72 | 86 | 40 |
| pglib_opf_case13659_pegase | 13659 | 20467 | 8.9480e+06 | 1.39 | 75 | 69 |

TABLE VII
AC-OPF BOUNDS ON PGLIB-OPF API NETWORKS.

| Test Case | $ N $ | $ E $ | \$/h AC | Gap (%) SOC | Runtime (sec.) AC | Runtime (sec.) SOC |
|--------------------------------------|-------|-------|------------|----------------|----------------------|-----------------------|
| Congested Operating Conditions (API) | | | | | | |
| pglib_opf_case3_lmbd_api | 3 | 3 | 1.1242e+04 | 9.32 | <1 | <1 |
| pglib_opf_case5_pjm_api | 5 | 6 | 7.6377e+04 | 4.09 | <1 | <1 |
| pglib_opf_case14_ieee_api | 14 | 20 | 5.9994e+03 | 5.13 | <1 | <1 |
| pglib_opf_case24_ieee_rts_api | 24 | 38 | 1.3495e+05 | 17.87 | <1 | <1 |
| pglib_opf_case30_as_api | 30 | 41 | 4.9962e+03 | 44.61 | <1 | <1 |
| pglib_opf_case30_fsr_api | 30 | 41 | 7.0115e+02 | 2.76 | <1 | <1 |
| pglib_opf_case30_ieee_api | 30 | 41 | 1.8044e+04 | 5.46 | <1 | <1 |
| pglib_opf_case39_epri_api | 39 | 46 | 2.4975e+05 | 1.74 | <1 | <1 |
| pglib_opf_case57_ieee_api | 57 | 80 | 4.9297e+04 | 0.09 | <1 | <1 |
| pglib_opf_case73_ieee_rts_api | 73 | 120 | 4.2273e+05 | 12.89 | <1 | <1 |
| pglib_opf_case89_pegase_api | 89 | 210 | 1.3428e+05 | 13.47 | <1 | <1 |
| pglib_opf_case118_ieee_api | 118 | 186 | 2.4205e+05 | 28.81 | <1 | <1 |
| pglib_opf_case162_ieee_dtc_api | 162 | 284 | 1.2100e+05 | 4.36 | <1 | <1 |
| pglib_opf_case179_goc_api | 179 | 263 | 1.9321e+06 | 9.88 | <1 | <1 |
| pglib_opf_case200_tamu_api | 200 | 245 | 3.7694e+04 | 0.02 | <1 | <1 |
| pglib_opf_case240_pserc_api | 240 | 448 | 4.7681e+06 | 0.74 | 4 | 2 |
| pglib_opf_case300_ieee_api | 300 | 411 | 6.5015e+05 | 0.89 | <1 | <1 |
| pglib_opf_case500_tamu_api | 500 | 597 | 4.0343e+04 | 0.08 | 2 | <1 |
| pglib_opf_case588_sdet_api | 588 | 686 | 4.0465e+05 | 0.76 | <1 | <1 |
| pglib_opf_case1354_pegase_api | 1354 | 1991 | 1.4867e+06 | 0.66 | 5 | 4 |
| pglib_opf_case1888_rte_api | 1888 | 2531 | 1.9674e+06 | 0.22 | 10 | 7 |
| pglib_opf_case1951_rte_api | 1951 | 2596 | 2.4459e+06 | 0.46 | 10 | 6 |
| pglib_opf_case2000_tamu_api | 2000 | 3206 | 1.2883e+06 | 2.49 | 18 | 4 |
| pglib_opf_case2316_sdet_api | 2316 | 3017 | 2.2057e+06 | 1.90 | 9 | 7 |
| pglib_opf_case2383wp_k_api | 2383 | 2896 | 2.7913e+05 | 0.01 | 3 | 2 |
| pglib_opf_case2736sp_k_api | 2736 | 3504 | 6.2162e+05 | 13.21 | 9 | 4 |
| pglib_opf_case2737sop_k_api | 2737 | 3506 | 3.6913e+05 | 6.39 | 8 | 2 |
| pglib_opf_case2746wop_k_api | 2746 | 3514 | 5.1166e+05 | 0.01 | 4 | 2 |
| pglib_opf_case2746wp_k_api | 2746 | 3514 | 5.8183e+05 | 0.00 | 5 | 2 |
| pglib_opf_case2848_rte_api | 2848 | 3776 | 1.4964e+06 | 0.23 | 33 | 7 |
| pglib_opf_case2853_sdet_api | 2853 | 3921 | 2.4547e+06 | 2.05 | 13 | 7 |
| pglib_opf_case2868_rte_api | 2868 | 3808 | 2.3282e+06 | 0.19 | 21 | 7 |
| pglib_opf_case2869_pegase_api | 2869 | 4582 | 2.9342e+06 | 1.33 | 15 | 9 |
| pglib_opf_case3012wp_k_api | 3012 | 3572 | 7.2887e+05 | 0.00 | 5 | 2 |
| pglib_opf_case3120sp_k_api | 3120 | 3693 | 9.6963e+05 | 24.18 | 14 | 5 |
| pglib_opf_case3375wp_k_api | 3374 | 4161 | 5.8609e+06 | — | 13 | 384 |
| pglib_opf_case4661_sdet_api | 4661 | 5997 | 2.7141e+06 | 2.70 | 19 | 15 |
| pglib_opf_case6468_rte_api | 6468 | 9000 | 2.3293e+06 | 0.62 | 70 | 187 |
| pglib_opf_case6470_rte_api | 6470 | 9005 | 2.6077e+06 | 0.64 | 53 | 24 |
| pglib_opf_case6495_rte_api | 6495 | 9019 | 3.1636e+06 | 3.91 | 63 | 26 |
| pglib_opf_case6515_rte_api | 6515 | 9037 | 3.1624e+06 | 2.19 | 70 | 25 |
| pglib_opf_case9241_pegase_api | 9241 | 16049 | 7.0265e+06 | — | 93 | 1563 |
| pglib_opf_case10000_tamu_api | 10000 | 12706 | 1.8164e+06 | 7.93 | 125 | 39 |
| pglib_opf_case13659_pegase_api | 13659 | 20467 | 9.2971e+06 | 1.83 | 80 | 83 |

OPF networks, an optimization problem is solved in order to find the minimum value of θ^Δ that can be applied on all of the branches in the network, while retaining a feasible AC power flow. Once this small value of θ^Δ is determined, the original test case is updated with this value, which introduces voltage angle difference congestion on the network branches. The results of the SAD networks are presented in Table VIII. Interestingly, this entirely different approach to modifying the base networks also leads to significant optimality gaps, with 75% of the SAD networks having optimality gaps above 1%. This suggest that many of these cases will be useful for benchmarking AC-OPF algorithms.

It is important to note that in all three result tables, the significant optimality gaps can be caused by two factors: (1) the heuristic for finding feasible AC-OPF solution fails to find the global optimum (e.g. see [61]); (2) the SOC convex relaxation is weak (e.g. see [5]) and does not provide a tight bound on the quality of the AC-OPF solution. Both factors present interesting avenues for research on AC-OPF algorithms.

VII. CONCLUSIONS

This report has highlighted some of the shortcomings of using existing network datasets for benchmarking AC Optimal Power Flow algorithms and has proposed the PGLIB-OPF networks to mitigate them. Leveraging data-driven models, PGLIB-OPF ensures that all of the networks have reasonable values for key power network parameters, including generation injection limits, generation costs, and branch thermal limits. Furthermore, the active power increase and small angle difference network variants are developed to provide additional challenging cases for benchmarking. A detailed validation study demonstrates that the majority of the PGLIB-OPF networks exhibit significant optimality gaps and are therefore useful for benchmarking AC-OPF algorithms.

It is important to emphasize that while the primary challenge of this work has been to develop realistic and challenging network datasets for benchmarking the AC-OPF problem presented in Model 1, there is still a significant gap in the models used for industry-grade AC optimal power flow studies [62]–[64]. Some of the key extensions include: information about configurable assets such as bus shunts, switches, and transformer tap settings; N-1 contingency cases; branch thermal limits for short- and long-term overloading; and generator capability curves. As the research community is able to addresses the challenges presented in the PGLIB-OPF networks, it is important to also consider more realistic extensions of Model 1 and to curate new PGLIB repositories for those model variants.

Although PGLIB-OPF has highlighted some advantages for AC-OPF benchmarking, its network datasets are still by-in-large synthetically generated. This highlights the continued

need for industry engagement in the development of more detailed and realistic network datasets for benchmarking AC-OPF algorithms. We hope that the PGLIB-OPF networks proposed herein will be sufficient for the research community to benchmark AC-OPF algorithms, while more real-world network datasets are developed and contributed to the PGLIB-OPF repository in the years to come.

APPENDIX EXTENSIONS AND ALTERNATIVE APPLICATIONS

While this report focuses on the AC-OPF formulation described in Model 1, there are a variety of possible modifications, extensions, and other problems that are relevant to many power system researchers. This appendix first presents common modifications of Model 1 and then summarizes several possible alternative uses of the PGLIB data.

A. Current Flow Limits

The OPF formulation in Model 1 considers line-flow limits that are based on apparent power (2h) and voltage angle differences (2i). A common modified problem formulation limits the magnitudes of the current flows on each line. Specifically, the following constraints either replace or augment the apparent power flow limits in (2h):

$$I_{lij} = \left(\mathbf{Y}_l + i \frac{\mathbf{b}_l^c}{2} \right) \frac{V_i}{|\mathbf{T}_l|^2} - \mathbf{Y}_l \frac{V_j}{\mathbf{T}_l^*} \quad \forall (l, i, j) \in E \quad (6a)$$

$$I_{lji} = \left(\mathbf{Y}_l + i \frac{\mathbf{b}_l^c}{2} \right) V_j - \mathbf{Y}_l \frac{V_i}{\mathbf{T}_l} \quad \forall (l, i, j) \in E \quad (6b)$$

$$|I_{lij}| \leq I_l^u \quad \forall (l, i, j) \in E \cup E^R \quad (6c)$$

Note that the per unit value of I_l^u is often assumed to be equivalent to the per unit value of s_l^u .

B. Branch Charging Model

The Π -circuit branch model of this work (i.e., Figure 1), only considers the susceptance impacts of line changing. After the inception of that MATPOWER data format, a number of commercial power flow tools now support the following, more general model, of line charging:

$$S_{lij} = (\mathbf{Y}_l + \mathbf{Y}_{lij}^c)^* \frac{|V_i|^2}{|\mathbf{T}_l|^2} - \mathbf{Y}_l^* \frac{V_i V_j^*}{\mathbf{T}_l} \quad \forall (l, i, j) \in E \quad (7a)$$

$$S_{lji} = (\mathbf{Y}_l + \mathbf{Y}_{lji}^c)^* |V_j|^2 - \mathbf{Y}_l^* \frac{V_i^* V_j}{\mathbf{T}_l^*} \quad \forall (l, i, j) \in E \quad (7b)$$

where the values \mathbf{Y}_{lij}^c and \mathbf{Y}_{lji}^c represent the line charging admittance on the *from* and *to* sides of the branch respectively. This model generalizes the branch model from Figure 1 by incorporating line charge conductance effects and asymmetrical charging effects.

TABLE VIII
AC-OPF BOUNDS ON PGLIB-OPF SAD NETWORKS.

| Test Case | $ N $ | $ E $ | \$/h AC | Gap (%) SOC | Runtime (sec.) AC | Runtime (sec.) SOC |
|---|-------|-------|------------|----------------|----------------------|-----------------------|
| Small Angle Difference Conditions (SAD) | | | | | | |
| pglib_opf_case3_lmbd_sad | 3 | 3 | 5.9593e+03 | 3.75 | <1 | <1 |
| pglib_opf_case5_pjm_sad | 5 | 6 | 2.6115e+04 | 3.62 | <1 | <1 |
| pglib_opf_case14_ieee_sad | 14 | 20 | 2.7773e+03 | 21.54 | <1 | <1 |
| pglib_opf_case24_ieee_rts_sad | 24 | 38 | 7.6943e+04 | 9.56 | <1 | <1 |
| pglib_opf_case30_as_sad | 30 | 41 | 8.9749e+02 | 7.88 | <1 | <1 |
| pglib_opf_case30_fsr_sad | 30 | 41 | 5.7679e+02 | 0.47 | <1 | <1 |
| pglib_opf_case30_ieee_sad | 30 | 41 | 8.2085e+03 | 9.70 | <1 | <1 |
| pglib_opf_case39_epri_sad | 39 | 46 | 1.4835e+05 | 0.66 | <1 | <1 |
| pglib_opf_case57_ieee_sad | 57 | 80 | 3.8664e+04 | 0.71 | <1 | <1 |
| pglib_opf_case73_ieee_rts_sad | 73 | 120 | 2.2775e+05 | 6.75 | <1 | <1 |
| pglib_opf_case89_pegase_sad | 89 | 210 | 1.0729e+05 | 0.73 | <1 | <1 |
| pglib_opf_case118_ieee_sad | 118 | 186 | 1.0522e+05 | 8.22 | <1 | <1 |
| pglib_opf_case162_ieee_dtc_sad | 162 | 284 | 1.0870e+05 | 6.48 | <1 | <1 |
| pglib_opf_case179_goc_sad | 179 | 263 | 7.6254e+05 | 1.12 | <1 | <1 |
| pglib_opf_case200_tamu_sad | 200 | 245 | 2.7558e+04 | 0.01 | <1 | <1 |
| pglib_opf_case240_pserc_sad | 240 | 448 | 3.4071e+06 | 4.98 | 4 | 2 |
| pglib_opf_case300_ieee_sad | 300 | 411 | 5.6571e+05 | 2.61 | <1 | <1 |
| pglib_opf_case500_tamu_sad | 500 | 597 | 7.9234e+04 | 7.92 | 2 | <1 |
| pglib_opf_case588_sdet_sad | 588 | 686 | 3.2986e+05 | 6.81 | 2 | <1 |
| pglib_opf_case1354_pegase_sad | 1354 | 1991 | 1.2588e+06 | 1.57 | 7 | 3 |
| pglib_opf_case1888_rte_sad | 1888 | 2531 | 1.4139e+06 | 2.82 | 11 | 29 |
| pglib_opf_case1951_rte_sad | 1951 | 2596 | 2.0928e+06 | 0.48 | 20 | 6 |
| pglib_opf_case2000_tamu_sad | 2000 | 3206 | 1.2303e+06 | 0.35 | 12 | 3 |
| pglib_opf_case2316_sdet_sad | 2316 | 3017 | 1.7753e+06 | 1.80 | 8 | 5 |
| pglib_opf_case2383wp_k_sad | 2383 | 2896 | 1.9127e+06 | 2.93 | 10 | 6 |
| pglib_opf_case2736sp_k_sad | 2736 | 3504 | 1.3273e+06 | 1.63 | 10 | 5 |
| pglib_opf_case2737sop_k_sad | 2737 | 3506 | 7.9153e+05 | 1.95 | 9 | 4 |
| pglib_opf_case2746wop_k_sad | 2746 | 3514 | 1.2343e+06 | 2.37 | 9 | 4 |
| pglib_opf_case2746wp_k_sad | 2746 | 3514 | 1.6676e+06 | 2.22 | 9 | 6 |
| pglib_opf_case2848_rte_sad | 2848 | 3776 | 1.2890e+06 | 0.26 | 21 | 7 |
| pglib_opf_case2853_sdet_sad | 2853 | 3921 | 2.0701e+06 | 1.74 | 11 | 7 |
| pglib_opf_case2868_rte_sad | 2868 | 3808 | 2.0224e+06 | 0.64 | 21 | 7 |
| pglib_opf_case2869_pegase_sad | 2869 | 4582 | 2.4689e+06 | 1.13 | 14 | 8 |
| pglib_opf_case3012wp_k_sad | 3012 | 3572 | 2.6213e+06 | 1.62 | 12 | 7 |
| pglib_opf_case3120sp_k_sad | 3120 | 3693 | 2.1755e+06 | 1.61 | 14 | 7 |
| pglib_opf_case3375wp_k_sad | 3374 | 4161 | 7.4382e+06 | 0.55 | 13 | 7 |
| pglib_opf_case4661_sdet_sad | 4661 | 5997 | 2.2610e+06 | 1.96 | 19 | 14 |
| pglib_opf_case6468_rte_sad | 6468 | 9000 | 2.0697e+06 | 1.12 | 72 | 35 |
| pglib_opf_case6470_rte_sad | 6470 | 9005 | 2.2416e+06 | 1.91 | 42 | 25 |
| pglib_opf_case6495_rte_sad | 6495 | 9019 | 3.0678e+06 | 15.11 | 80 | 27 |
| pglib_opf_case6515_rte_sad | 6515 | 9037 | 2.8826e+06 | 8.26 | 69 | 25 |
| pglib_opf_case9241_pegase_sad | 9241 | 16049 | 6.3195e+06 | 2.48 | 92 | 39 |
| pglib_opf_case10000_tamu_sad | 10000 | 12706 | 2.4859e+06 | 0.72 | 70 | 38 |
| pglib_opf_case13659_pegase_sad | 13659 | 20467 | 9.0433e+06 | 1.69 | 75 | 45 |

C. Generator Capability Curves

Model 1 represents generators with box constraints that independently limit active and reactive power outputs. A more detailed model recognizes that the current flows inside of a generator are jointly dependent on both the active and reactive power outputs. The generator must be operated to limit the heating caused by these internal current flows. Thus, the more detailed “capability curve” generator model (also known as a “D-curve” model) forms generator limits that couple the active and reactive power outputs [65]. Estimates of the additional data needed for the generator capability curve model can be extracted from the box constraints on active and reactive power injections provided in typical datasets [66], [67]. Additionally, the MATPOWER data format is capable of representing a piecewise-linear approximation of the generator capability curve model [16].

D. Voltage & Reactive Power Control

In practice, reactive power management devices, such as bus shunts and transformer taps, play a critical role in managing the voltage profile of an AC power network and improving power quality in congested parts of a network [68]. A notable limitation of the OPF formulation presented in Model 1 is the limited amount of reactive power control devices, which may bias the feasible solutions to a specific voltage profile provided with the network data. At this time, extensions of the Model 1 that consider reactive power controls are an active area of research with promising initial results [45], [69]–[71]. However, a variety of subtle challenges arise when incorporating such devices into an OPF problem formulation [63] and continued research is required to arrive at a broadly accepted generalization of Model 1 that incorporates more reactive control devices.

E. Other Problem Formulations

The OPF formulation in Model 1 considers a single period of steady-state power system behavior. Power system engineers solve a wide variety of other optimization and control problems relevant to the design and operation of power systems [72]–[74]. Formulating many of these problems requires augmenting the data available in PGLIB-OPF with other information. Table IX summarizes several other classes of optimization and control problems, indicates examples of information that may be required for these problems beyond the data provided in PGLIB-OPF, and provides selected references for each class of problems. While currently beyond the scope of this effort, extension of PGLIB to incorporate the data necessary for test cases that are applicable to these and other classes of problems is an important topic for future work.

REFERENCES

- [1] C. Coffrin and P. Van Hentenryck, “A linear-programming approximation of AC power flows,” *INFORMS Journal on Computing*, vol. 26, no. 4, pp. 718–734, 2014. [Online]. Available: <http://dx.doi.org/10.1287/ijoc.2014.0594>
- [2] R. P. O’Neill, A. Castillo, and M. B. Cain, “The IV formulation and linear approximations of the AC optimal power flow problem,” Published online at <http://www.ferc.gov/industries/electric/indus-act/market-planning/opf-papers/acopf-2-iv-linearization.pdf>, December 2012, accessed: 18/11/2013.
- [3] R. A. Jabr, “Radial distribution load flow using conic programming,” *IEEE Transactions on Power Systems*, vol. 21, no. 3, pp. 1458–1459, Aug. 2006.
- [4] M. Farivar, C. R. Clarke, S. H. Low, and K. M. Chandy, “Inverter VAR control for distribution systems with renewables,” in *2011 IEEE International Conference on Smart Grid Communications (SmartGridComm)*, Oct 2011, pp. 457–462.
- [5] C. Coffrin, H. L. Hijazi, and P. V. Hentenryck, “The QC relaxation: A theoretical and computational study on optimal power flow,” *IEEE Transactions on Power Systems*, vol. 31, no. 4, pp. 3008–3018, July 2016.
- [6] H. Hijazi, C. Coffrin, and P. V. Hentenryck, “Convex quadratic relaxations for mixed-integer nonlinear programs in power systems,” *Mathematical Programming Computation*, vol. 9, no. 3, pp. 321–367, Sept. 2017.
- [7] X. Bai, H. Wei, K. Fujisawa, and Y. Wang, “Semidefinite programming for optimal power flow problems,” *International Journal of Electrical Power & Energy Systems*, vol. 30, no. 6-7, pp. 383 – 392, 2008.
- [8] D. Molzahn and I. Hiskens, “Moment-based relaxation of the optimal power flow problem,” in *Power Systems Computation Conference (PSCC)*, 2014, Aug. 2014, pp. 1–7.
- [9] B. Ghaddar, J. Marecek, and M. Mevissen, “Optimal power flow as a polynomial optimization problem,” *IEEE Transactions on Power Systems*, vol. 31, no. 1, pp. 539–546, Jan. 2016.
- [10] D. K. Molzahn and I. A. Hiskens, “Sparsity-exploiting moment-based relaxations of the optimal power flow problem,” *IEEE Transactions on Power Systems*, vol. 30, no. 6, pp. 3168–3180, Nov. 2015.
- [11] C. Josz and D. K. Molzahn, “Lasserre hierarchy for large scale polynomial optimization in real and complex variables,” *SIAM Journal on Optimization*, vol. 28, no. 2, pp. 1017–1048, 2018.
- [12] C. Coffrin and L. A. Roald, “Convex relaxations in power system optimization: A brief introduction,” *arXiv:1807.07227*, July 2018, videos available at https://www.youtube.com/watch?v=gB43TmcoUpA&list=PLEuOzWTGxj2ZZ_XUutDwNFvNfSWwWCgR5.
- [13] G. Wang and H. Hijazi, “Mathematical programming methods for microgrid design and operations: A survey on deterministic and stochastic approaches,” *Computational Optimization and Applications*, June 2018.
- [14] D. K. Molzahn and I. A. Hiskens, “A survey of relaxations and approximations of the power flow equations,” *Foundations and Trends in Electric Energy Systems*, vol. 4, no. 1-2, pp. 1–221, Feb. 2019.
- [15] J. Lavaei and S. H. Low, “Zero duality gap in optimal power flow problem,” *IEEE Transactions on Power Systems*, vol. 27, no. 1, pp. 92 –107, Feb. 2012.
- [16] R. D. Zimmerman, C. E. Murillo-Sandnchez, and R. J. Thomas, “Matpower: Steady-state operations, planning, and analysis tools for power systems research and education,” *IEEE Transactions on Power Systems*, vol. 26, no. 1, pp. 12 –19, Feb. 2011.
- [17] Gurobi Optimization, Inc., “Gurobi optimizer reference manual,” Published online at <http://www.gurobi.com>, 2014.
- [18] I. IBM, “IBM ILOG CPLEX Optimization Studio,” <http://www-01.ibm.com/software/commerce/optimization/cplex-optimizer/>, 2014.
- [19] MOSEK ApS, *The MOSEK optimization toolbox*, 2015. [Online]. Available: <http://www.mosek.com/resources/doc>
- [20] J. L. Carpentier, “Contribution a l’Etude du Dispatching Economique,” *Bulletin de la Societe Francaise des Electriciens*, vol. 8, no. 3, pp. 431–447, 1962.
- [21] J. Momoh, R. Adapa, and M. El-Hawary, “A review of selected optimal power flow literature to 1993. I. Nonlinear and quadratic programming

TABLE IX
OTHER PROBLEM FORMULATIONS

| Problem | Description | Additional Information Required | Refs. |
|---|--|--|-------------------|
| Power Flow | Determine a voltage profile corresponding to a specified set of power injections and voltage magnitudes. | <ul style="list-style-type: none"> Bus type specifications (PV, PQ, Slack) for each bus. Active power injections for PV and PQ buses. Reactive power injections for PQ buses. Voltage magnitudes for the slack bus and PV buses. | [75], [76] |
| Multi-Period OPF | Extend the single-period OPF formulation of Model 1 to multiple periods with time-varying load demands and energy storage models. | <ul style="list-style-type: none"> Time-varying load demands and renewable generation. Generator ramp rates. Models of energy storage devices. | [41], [77] |
| Unit Commitment | Schedule generator on/off statuses and power outputs considering costs and constraints associated with operating, starting up, and shutting down generators. | <ul style="list-style-type: none"> Time-varying load demands and renewable generation. Generator start-up and shut-down costs, ramp rates, minimum run times, and minimum down times. Models of energy storage devices. | [78]–[81] |
| Network Reconfiguration | Optimize the topology of a transmission or distribution network by changing the statuses of switches. | <ul style="list-style-type: none"> Locations of switches. | [24], [82], [83] |
| State Estimation | Determine the operating point that minimizes a weighted error metric for a given set of measurements. | <ul style="list-style-type: none"> Locations and values for the measurements. Characterizations of measurement noise. | [84]–[86] |
| Voltage Stability Analyses | Compute various margins to the system's loadability limit. | <ul style="list-style-type: none"> Models for variations in the load demands and generator outputs. Models for the actions of voltage control devices such as switched shunt capacitors and tap-changing transformers. | [87], [88] |
| Small-Signal Dynamic Stability Analyses | Simulate or analytically characterize the behavior of a power system subject to small perturbations. | <ul style="list-style-type: none"> Dynamical models for devices such as generators and loads, often represented as a system of differential-algebraic equations. Models for the perturbations. | [89] |
| Transient Stability Analyses | Simulate or analytically characterize the behavior of a power system following a large disturbance. | <ul style="list-style-type: none"> Dynamical models for devices such as generators and loads, often represented as a system of differential-algebraic equations. Models for the disturbances. | [89]–[91] |
| Cascading Failure Analyses | Simulate and analyze the processes by which failures of certain system devices can lead to cascades of subsequent failures. | <ul style="list-style-type: none"> Models relating overload amounts to the failure probabilities of each device. System responses to failures of various devices. | [92] |
| Reliability Analyses and Expansion Planning | Compute estimates of reliability metrics such as loss of load probability. Identify investments in new devices such as generators and transmission lines that facilitate reliable operation. | <ul style="list-style-type: none"> Multiple snapshots of load demands representing time-series or scenario data. Failure rates for various devices such as generators and lines. | [25], [41], [93] |
| Coupled Transmission / Distribution System Analyses | Analyses that jointly consider models of transmission and distribution systems. | <ul style="list-style-type: none"> Distribution system models, possibly with three-phase unbalanced network representations. Model for the couplings between the transmission and distribution systems. | [94]–[96] |
| Coupled Infrastructure Analyses | Analyses of electric power systems coupled with other networks such as natural gas, water, transportation, and communication systems. | <ul style="list-style-type: none"> Models for the other infrastructures and their couplings with the electric grid. | [97]–[99] |
| Stochastic Formulations | Problem variants that consider uncertainty, often with respect to the power injections. | <ul style="list-style-type: none"> Models of the uncertainty characteristics. Recourse models describing how each device responds to the uncertainty realizations. | [13], [80], [100] |
| Distributed Formulations | Problem variants that use distributed rather than centralized formulations. | <ul style="list-style-type: none"> Models of the communications among the distributed agents that work together to solve the problem. | [86], [101] |
| Contingency-Constrained Formulations | Problem variants that ensure the security of system operations after the occurrence of certain contingencies. | <ul style="list-style-type: none"> A list of contingencies. Recourse models describing how each device responds to the contingency. | [62]–[64] |

approaches,” *IEEE Transactions on Power Systems*, vol. 14, no. 1, pp. 96–104, Feb. 1999.

[22] J. Momoh, M. El-Hawary, and R. Adapa, “A review of selected optimal power flow literature to 1993. II. Newton, linear programming and interior point methods,” *IEEE Transactions on Power Systems*, vol. 14, no. 1, pp. 105–111, Feb. 1999.

[23] A. Castillo and R. P. O’Neill, “Survey of approaches to solving the acopf (opf paper 4),” US Federal Energy Regulatory Commission, Tech. Rep., Mar. 2013.

[24] E. Fisher, R. O’Neill, and M. Ferris, “Optimal transmission switching,” *IEEE Transactions on Power Systems*, vol. 23, no. 3, pp. 1346–1355, 2008.

[25] R. Jabr, “Optimization of AC transmission system planning,” *IEEE Transactions on Power Systems*, vol. 28, no. 3, pp. 2779–2787, Aug. 2013.

[26] H. Mittelmann, “Benchmarks for optimization software,” Published online at <http://plato.la.asu.edu/bench.html>, accessed: 24/11/2014.

[27] University of Washington, Dept. of Electrical Engineering, “Power systems test case archive,” Published online at <http://www.ee.washington.edu/research/pstca/>, 1999, accessed: 30/04/2012.

[28] T. Heidel, K. Hedman, and P. McGrath, “Generating realistic information for the development of distribution and transmission algorithms (GRID DATA),” Published online at <https://arpa-e.energy.gov/?q=arpa-e-programs/grid-data>, January 2016, accessed: 08/08/2018.

[29] A. Verma, “Power grid security analysis: An optimization approach,” Ph.D. dissertation, Columbia University, 2009.

[30] K. Lehmann, A. Grastien, and P. V. Hentenryck, “AC-feasibility on tree networks is NP-hard,” *IEEE Transactions on Power Systems*, vol. 31,

no. 1, pp. 798–801, Jan. 2016.

[31] B. Lesieutre, D. Molzahn, A. Borden, and C. DeMarco, “Examining the limits of the application of semidefinite programming to power flow problems,” in *49th Annual Allerton Conference on Communication, Control, and Computing (Allerton), 2011*, Sept. 2011, pp. 1492–1499.

[32] F. Li and R. Bo, “Small test systems for power system economic studies,” in *Power and Energy Society General Meeting, 2010 IEEE*, July 2010, pp. 1–4.

[33] O. Alsac and B. Stott, “Optimal load flow with steady-state security,” *IEEE Transactions on Power Apparatus and Systems*, vol. PAS-93, no. 3, pp. 745–751, May 1974.

[34] R. W. Ferrero, S. M. Shahidehpour, and V. C. Ramesh, “Transaction analysis in deregulated power systems using game theory,” *IEEE Transactions on Power Systems*, vol. 12, no. 3, pp. 1340–1347, Aug. 1997.

[35] G. Bills, “On-line stability analysis study, RP 90-1,” Request online at <http://www.osti.gov/scitech/biblio/5984031>, Oct. 1970.

[36] A. Pai, *Energy Function Analysis for Power System Stability*, ser. Kluwer International Series in Engineering and Computer Science. Springer, 1989.

[37] C. M. Ferreira, F. P. M. Barbosa, and C. I. F. Agreira, “Transient stability preventive control of an electric power system using a hybrid method,” in *12th International Middle-East Power System Conference (MEPCON)*, Mar. 2008, pp. 141–145.

[38] Power Systems Engineering Research Center, “Transfer capability calculator,” Published online at <http://www.pserc.cornell.edu/tcc/>, 2001, accessed: 25/08/2014.

[39] P. F. Albrecht, M. P. Bhavaraju, B. E. Biggerstaff, R. Billinton, G. Elsoe Jorgensen, N. D. Reppen, and P. B. Shortley, “IEEE reliability test system. A report prepared by the reliability test system task force of the application of probability methods subcommittee,” *IEEE Transactions on Power Apparatus and Systems*, vol. PAS-98, no. 6, pp. 2047–2054, Nov. 1979.

[40] Power Systems Control and Automation Laboratory, “IEEE 24-substation reliability test system, generator data,” Published online at <http://pscal.ece.gatech.edu/testsys/generators.html>, accessed: 22/10/2013.

[41] C. Grigg, P. Wong, P. Albrecht, R. Allan, M. Bhavaraju, R. Billinton, Q. Chen, C. Fong, S. Haddad, S. Kuruganty, W. Li, R. Mukerji, D. Patton, N. Rau, D. Reppen, A. Schneider, M. Shahidehpour, and C. Singh, “The IEEE reliability test system-1996. A report prepared by the reliability test system task force of the application of probability methods subcommittee,” *IEEE Trans. Power Syst.*, vol. 14, no. 3, pp. 1010–1020, Aug. 1999.

[42] C. Josz, S. Fliscounakis, J. Maeght, and P. Panciatici, “AC power flow data in MATPOWER and QCQP format: iTesla, RTE snapshots, and PEGASE,” *CoRR*, vol. abs/1603.01533, 2016. [Online]. Available: <https://arxiv.org/abs/1603.01533>

[43] A. B. Birchfield, T. Xu, K. M. Gegner, K. S. Shetye, and T. J. Overbye, “Grid structural characteristics as validation criteria for synthetic networks,” *IEEE Transactions on Power Systems*, vol. 32, no. 4, pp. 3258–3265, July 2017.

[44] Sustainable Data Evolution Technology, “SDET transmission models,” Published online at <https://egriddata.org/group/sustainable-data-evolution-technology-sdet>, 2018, accessed: 07/31/2018.

[45] Grid Optimization Competition, “Grid optimization competition datasets,” Published online at <https://gocompetition.energy.gov/competition/beta/?page=data>, 2018, accessed: 07/31/2018.

[46] J. E. Price and J. Goodin, “Reduced network modeling of wecc as a market design prototype,” in *2011 IEEE Power and Energy Society General Meeting*, July 2011, pp. 1–6.

[47] Power Systems Engineering Research Center, “Completed projects, M-21,” Published online at https://pserc.wisc.edu/research/public_reports.aspx, 2018, accessed: 07/31/2018.

[48] R. D. Zimmerman and C. E. Murillo-Sánchez, “Matpower,” Dec. 2016. [Online]. Available: <https://doi.org/10.5281/zenodo.3237810>

[49] A. Wächter and L. T. Biegler, “On the implementation of a primal-dual interior point filter line search algorithm for large-scale nonlinear programming,” *Mathematical Programming*, vol. 106, no. 1, pp. 25–57, 2006.

[50] Research Councils U.K., “The HSL mathematical software library,” Published online at <http://www.hsl.rl.ac.uk/>, accessed: 30/10/2014.

[51] C. Coffrin, R. Bent, K. Sundar, Y. Ng, and M. Lubin, “Powermodels.jl: An open-source framework for exploring power flow formulations,” in *2018 Power Systems Computation Conference (PSCC)*, June 2018, pp. 1–8.

[52] C. Coffrin, D. Gordon, and P. Scott, “NESTA, The NICTA Energy System Test Case Archive,” *CoRR*, vol. abs/1411.0359, 2014. [Online]. Available: <http://arxiv.org/abs/1411.0359>

[53] U.S. Energy Information Administration, “Annual electric generator data - eia-860 data file,” Published online at www.eia.gov/electricity/data/eia860/, 2012, accessed: 25/08/2014.

[54] —, “State Energy Data System (SEDS): 1960-2012 (complete),” Published online at <http://www.eia.gov/state/seds/seds-data-complete.cfm>, 2012, accessed: 25/08/2014.

[55] —, “Table 8.2 Average tested heat rates by prime mover and energy source, 2007–2016, from EIA-860, Annual electric generator report,” Published online at https://www.eia.gov/electricity/annual/html/epa_08_02.html, 2016, accessed: 29/09/2018.

[56] P. Kundur, *Power System Stability and Control*. McGraw-Hill Professional, 1994.

[57] C. Coffrin, P. Van Hentenryck, and R. Bent, “Accurate load and generation scheduling for linearized DC models with contingencies,” in *IEEE Power and Energy Society General Meeting*, July 2012, pp. 1–8.

[58] C. Coffrin, H. L. Hijazi, and P. V. Hentenryck, “Strengthening the SDP relaxation of AC power flows with convex envelopes, bound tightening, and valid inequalities,” *IEEE Transactions on Power Systems*, vol. 32, no. 5, pp. 3549–3558, Sept. 2017.

[59] C. Coffrin, H. Hijazi, K. Lehmann, and P. Van Hentenryck, “Primal and dual bounds for optimal transmission switching,” *Power Systems Computation Conference (PSCC)*, pp. 1–8, 08 2014.

[60] T. Potluri and K. W. Hedman, “Impacts of topology control on the ACOPF,” in *IEEE Power and Energy Society General Meeting*, 2012, pp. 1–7.

[61] W. Bukhsh, A. Grothey, K. McKinnon, and P. Trodden, “Local solutions of the optimal power flow problem,” *IEEE Transactions on Power Systems*, vol. 28, no. 4, pp. 4780–4788, Nov 2013.

[62] B. Stott, O. Alsac, and A. J. Monticelli, “Security Analysis and Optimization,” *Proceedings of the IEEE*, vol. 75, no. 12, pp. 1623–1644, December 1987.

[63] B. Stott and O. Alsac, “Optimal power flow — Basic requirements for real-life problems and their solutions,” self published, available from brianstott@ieee.org, July 2012.

[64] F. Capitanescu, “Critical review of recent advances and further developments needed in AC optimal power flow,” *Electric Power Systems Research*, vol. 136, pp. 57–68, 2016.

[65] J. Y. Jackson, “Interpretation and use of generator reactive capability diagrams,” *IEEE Transactions on Industry and General Applications*, vol. IGA-7, no. 6, pp. 729–732, November 1971.

[66] D. K. Molzahn, Z. B. Friedman, B. C. Lesieutre, C. L. DeMarco, and M. C. Ferris, “Estimation of constraint parameters in optimal power flow data sets,” in *47th North American Power Symposium (NAPS)*, October 2015.

[67] B. Park, L. Tang, M. C. Ferris, and C. L. DeMarco, “Examination of three different ACOPF formulations with generator capability curves,” *IEEE Transactions on Power Systems*, vol. 32, no. 4, pp. 2913–2923, July 2017.

[68] M. Ilić, S. Cvijić, J. H. Lang, and J. Tong, “Optimal voltage management for enhancing electricity market efficiency,” in *IEEE Power Energy Society General Meeting*, July 2015, pp. 1–5.

[69] K. Y. Lee, I. Erlich, J. L. Rueda, and S. Wildenhues, “IEEE PES Competition on Application of Modern Heuristic Optimization Algorithms for Solving Optimal Power Flow Problems,” Published online at <http://sites.ieee.org/pes-iss/working-groups/>, 2013, accessed: 25/08/2014.

[70] M. Ruiz, J. Maeght, A. Mari, P. Panciatici, and A. Renaud, “A progressive method to solve large-scale AC optimal power flow with

discrete variables and control of the feasibility," in *Power Systems Computation Conference (PSCC)*, Aug. 2014, pp. 1–7.

[71] C. Coffrin and H. L. Hijazi, "Heuristic MINLP for optimal power flow problems," *Application of Modern Heuristic Optimization Algorithms for Solving Optimal Power Flow Problems Competition, 2014 IEEE Power & Energy Society General Meeting (PES)*, 2014.

[72] A. M. Sasson and H. M. Merrill, "Some applications of optimization techniques to power systems problems," *Proceedings of the IEEE*, vol. 62, no. 7, pp. 959–972, July 1974.

[73] J. A. Momoh, *Electric Power System Applications of Optimization*. CRC Press, 2008.

[74] A. J. Wood, B. F. Wollenberg, and G. B. Sheble, *Power Generation, Operation and Control*, 3rd ed. John Wiley and Sons, Inc., 2013.

[75] B. Stott, "Review of load-flow calculation methods," *Proceedings of the IEEE*, vol. 62, no. 7, pp. 916–929, July 1974.

[76] D. Mehta, D. K. Molzahn, and K. Turitsyn, "Recent advances in computational methods for the power flow equations," in *American Control Conference (ACC)*, Boston, MA, USA, July 2016, pp. 1753–1765.

[77] N. Alguacil and A. J. Conejo, "Multiperiod optimal power flow using Benders decomposition," *IEEE Transactions on Power Systems*, vol. 15, no. 1, pp. 196–201, February 2000.

[78] S. Sen and D. P. Kothari, "Optimal thermal generating unit commitment: A review," *International Journal of Electrical Power & Energy Systems*, vol. 20, no. 7, pp. 443–451, 1998.

[79] N. P. Padhy, "Unit commitment—A bibliographical survey," *IEEE Transactions on Power Systems*, vol. 19, no. 2, pp. 1196–1205, May 2004.

[80] M. Tahanan, W. Van Ackooij, A. Frangioni, and F. Lacalandra, "Large-scale unit commitment under uncertainty," *4OR*, vol. 13, no. 2, pp. 115–171, 2015.

[81] B. Kneueven, J. Ostrowski, and J. Watson, "On mixed integer programming formulations for the unit commitment problem," *Preprint*, http://www.optimization-online.org/DB_HTML/2018/11/6930.html, Nov. 2018.

[82] K. W. Hedman, S. S. Oren, and R. P. O'Neill, "A review of transmission switching and network topology optimization," in *IEEE Power & Energy Society General Meeting*, July 2011, pp. 1–7.

[83] H. L. Hijazi and S. Thiébaux, "Optimal AC distribution systems reconfiguration," in *Power Systems Computation Conference (PSCC)*, Wroclaw, Poland, August 2014.

[84] F. F. Wu, "Power system state estimation: A survey," *International Journal of Electrical Power & Energy Systems*, vol. 12, no. 2, pp. 80–87, 1990.

[85] A. Abur and A. Gómez Expósito, *Power System State Estimation: Theory and Implementation*. Marcel Dekker, 2004.

[86] V. Kekatos, G. Wang, H. Zhu, and G. B. Giannakis, "PSSE redux: Convex relaxation, decentralized, robust, and dynamic approaches," *arXiv:1708.03981*, August 2017.

[87] C. W. Taylor, *Power System Voltage Stability*. McGraw-Hill, 1994.

[88] I. Dobson, T. Van Cutsem, C. Vournas, C. L. DeMarco, M. Venkatasubramanian, T. Overbye, and C. A. Canizares, "Voltage stability assessment: Concepts, practices and tools," IEEE Power Engineering Society, Power System Stability Subcommittee Special Publication SP101PSS, August 2002.

[89] P. W. Sauer and M. A. Pai, *Power System Dynamics and Stability*. Prentice Hall, 1998.

[90] S. Abhyankar, G. Geng, M. Anitescu, X. Wang, and V. Dinavahi, "Solution Techniques for Transient Stability-Constrained Optimal Power Flow – Part I," *IET Generation, Transmission & Distribution*, vol. 11, pp. 3177–3185, August 2017.

[91] G. Geng, S. Abhyankar, X. Wang, and V. Dinavahi, "Solution Techniques for Transient Stability-Constrained Optimal Power Flow – Part II," *IET Generation, Transmission & Distribution*, vol. 11, pp. 3186–3193, August 2017.

[92] M. Vaiman, K. Bell, Y. Chen, B. Chowdhury, I. A. Dobson, P. Hines, M. Papic, S. Miller, and P. Zhang, "Risk assessment of cascading outages: Methodologies and challenges," *IEEE Transactions on Power Systems*, vol. 27, no. 2, pp. 631–641, May 2012.

[93] R. Romero, A. Monticelli, A. Garcia, and S. Haffner, "Test systems and mathematical models for transmission network expansion planning," *IEE Proceedings - Generation, Transmission and Distribution*, vol. 149, no. 1, pp. 27–36, January 2002.

[94] P. Aristidou and T. Van Cutsem, "Dynamic simulations of combined transmission and distribution systems using parallel processing techniques," in *Power Systems Computation Conference (PSCC)*, August 2014, pp. 1–7.

[95] B. Palmintier, E. Hale, B. Hodge, K. Baker, and T. M. Hansen, "Experiences integrating transmission and distribution simulations for DERs with the Integrated Grid Modeling System (IGMS)," in *Power Systems Computation Conference (PSCC)*, June 2016, pp. 1–7.

[96] K. Balasubramaniam and S. Abhyankar, "A combined transmission and distribution system co-simulation framework for assessing the impact of Volt/VAR control on transmission system," in *IEEE Power Energy Society General Meeting*, July 2017, pp. 1–5.

[97] S. K. Khaitan and J. D. McCalley, "Cyber physical system approach for design of power grids: A survey," in *IEEE Power Energy Society General Meeting*, July 2013, pp. 1–5.

[98] A. Zlotnik, L. A. Roald, S. Backhaus, M. Chertkov, and G. Andersson, "Coordinated scheduling for interdependent electric power and natural gas infrastructures," *IEEE Transactions on Power Systems*, vol. 32, no. 1, pp. 600–610, Jan. 2017.

[99] A. S. Zamzam, E. Dall'Anese, C. Zhao, J. A. Taylor, and N. Sidiropoulos, "Optimal water-power flow problem: Formulation and distributed optimal solution," *IEEE Transactions on Control of Network Systems*, vol. 6, no. 1, pp. 37–47, Mar. 2019.

[100] D. Bienstock, M. Chertkov, and S. Harnett, "Chance-constrained optimal power flow: Risk-aware network control under uncertainty," *SIAM Review*, vol. 56, no. 3, pp. 461–495, 2014.

[101] D. Molzahn, F. Dörfler, H. Sandberg, S. H. Low, S. Chakrabarti, R. Baldick, and J. Lavaei, "A survey of distributed optimization and control algorithms for electric power systems," *IEEE Transactions on Smart Grid*, vol. 8, no. 6, pp. 2939–2940, Nov. 2017.

LA-UR-18-29054